

Heat capacity at the field-induced ferromagnetic transition in $\text{Eu}_{0.58}\text{Sr}_{0.42}\text{MnO}_3$

G. J. Liu, J. R. Sun,^{a)} Y. W. Xie, D. J. Wang, C. M. Xiong, H. W. Zhang, T. Y. Zhao, and B. G. Shen

State Key Laboratory for Magnetism, Institute of Physics and Center for Condensed Matter Physics, Chinese Academy of Sciences, Beijing 100080, People's Republic of China

(Received 6 June 2005; accepted 9 September 2005; published online 27 October 2005)

$\text{Eu}_{0.58}\text{Sr}_{0.42}\text{MnO}_3$ is found to own a wide variety of magnetic structures, and two subsequent magnetic transitions, a PM-AFM (paramagnetic-antiferromagnetic) transition followed by an AFM-FM (ferromagnetic) transition, are observed under proper magnetic field. It is found that the thermal response of heat capacity to the AFM-FM transition is negligibly small when this transition is well below the PM-AFM transition, and grows rapidly as the Curie temperature sweeps through the broad PM-AFM transition under the driving of magnetic field. This result indicates that the magnetic anomaly in heat capacity comes exclusively from the PM-FM transition, and the field-induced AFM-FM transition has essentially no thermal effects. A qualitative explanation for this result has been given based on the mean field theory. © 2005 American Institute of Physics. [DOI: 10.1063/1.2125127]

Manganites have received much attention in the last decade because of their dramatic behaviors arising from the strong coupling among spin, charge, and orbital degrees of freedom.¹⁻³ It has been well known that the ferromagnetic (FM) to paramagnetic (PM) transition in the manganites always takes place accompanied by a metal to insulator transition, and the modification of magnetic field to the former produces a magnetoresistance effect.

In fact, in addition to resistivity, a thermal response to the magnetic transition is also expected due to the variation of exchange energy, and it can result in the excessive heat capacity of the form $C \propto MdM/dT$, where M is magnetization. This implies that any changes in magnetic order should have a thermal signature.⁴ Magnetic contribution to heat capacity has indeed been observed in manganese oxides, and the typical entropy change due to the FM transition is ~ 1.6 J/mol K as observed in the optimally hole-doped manganites such as $\text{La}_{0.7}\text{Ca}_{0.3}\text{MnO}_3$ and $\text{La}_{0.7}\text{Sr}_{0.3}\text{MnO}_3$.⁵

Exceptions are found in the manganite that experiences phase separation. It has been reported that there are two magnetic transitions, respectively at ~ 100 and ~ 220 K, in phase-separated $\text{La}_{1-x-y}(\text{Pr}, \text{Nd})_x\text{Ca}_y\text{MnO}_3$.⁶ It is surprising that no visible thermal anomalies were detected for the phase transition at ~ 100 K. As a qualitative explanation, Kiryukhin and collaborators suggested the percolation nature of this transition.⁷ This explanation is obviously not enough to justify this phenomenon, and many researchers revisited this problem in recent years. As an alternative, Raychaudhuri *et al.* studied the heat capacity of a single crystal $\text{Pr}_{0.63}\text{Ca}_{0.37}\text{MnO}_3$, and declared the occurrence of thermal anomaly associated with a field-induced magnetic transition at ~ 80 K.⁸ Hardy *et al.* subsequently found, without explanation, that doping minor Ga into the Mn sites of $\text{Pr}_{0.5}\text{Ca}_{0.5}\text{MnO}_3$ can arouse the magnetic contribution to heat capacity.⁹

In spite of the intensive studies, it is still not very clear why and when the thermal abnormal will appear, which is a problem concerning a thorough understanding of the magnetic transition in various circumstances such as phase-separated or other magnetic backgrounds. We noticed that $\text{Eu}_{0.58}\text{Sr}_{0.42}\text{MnO}_3$ exhibited complex, yet field-sensitive, magnetic structures.¹⁰ It is therefore an idealized sample for relevant studies.

The polycrystalline sample $\text{Eu}_{0.58}\text{Sr}_{0.42}\text{MnO}_3$ (ESMO) has been prepared by the solid-state-reaction method. The well-mixed stoichiometric mixture of Eu_2O_3 , SrCO_3 and MnCO_3 was first calcined at 1000°C for 24 h then at 1250°C for 48 h in air, with an intermediate grinding. The product thus obtained was reground, palletized, and sintered at 1350°C for another 36 h then furnace cooled to room temperature. The Rietveld refinement (space group $Pbnm$) of the x-ray diffraction spectrum, collected at the ambient temperature by a Rigaku x-ray diffractometer with a rotating anode, indicated that the sample is single phase of the orthorhombic structure with the lattice parameters of $a=5.4320$ Å, $b=5.4273$ Å and $c=7.6583$ Å.

Magnetization and resistivity measurements were performed on a superconducting quantum interference device magnetometer (MPMS-7), and the calorimetric measurement was conducted by a Physical Property Measurement System (PPMS-14H). All the data were collected in the warming process after zero-field cooling the sample to predetermined temperatures.

Figure 1 shows the temperature-dependent magnetization of ESMO measured under different magnetic fields. The sample is PM above ~ 100 K and antiferromagnetic (AFM) below ~ 90 K, as will be seen below, under low fields. The magnetic structure of ESMO is rather sensitive to external field, and a field of 1.5 T can effectively drive the system from the AFM state into the FM state. In this case a PM-AFM and an AFM-FM transition take place in sequence with decreasing temperature. When the applied field exceeds 4 T, the AFM phase is completely suppressed and system remains FM down to the lowest temperature. It should be noted that a

^{a)} Author to whom correspondence should be addressed; electronic mail: jrsun@g203.iphys.ac.cn

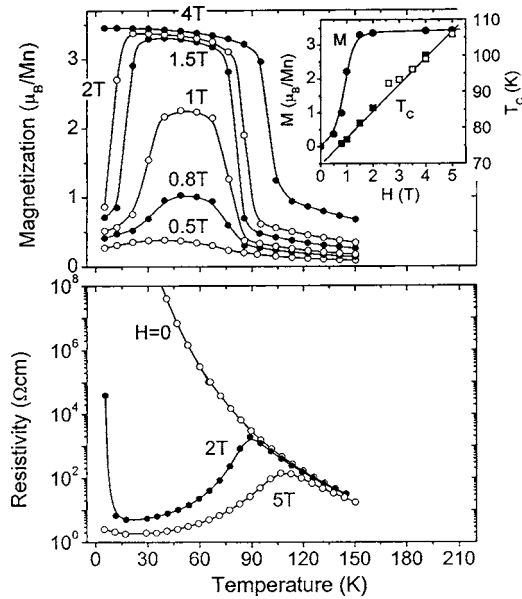


FIG. 1. Temperature-dependent magnetization of $\text{Eu}_{0.58}\text{Sr}_{0.42}\text{MnO}_3$ measured under different magnetic fields (top panel), and the corresponding resistivity (bottom panel). Inset plot shows the variation of magnetization ($T=45$ K) and Curie temperature with magnetic field. White squares denote the T_c determined by heat capacity. Solid lines are guides for the eye.

field of 1.5 T almost causes a full magnetic saturation. A simple calculation indicated that the magnetization is $\sim 3.3 \mu_B/\text{Mn}$ for $H=1.5$ T, while the theoretical value is $3.58 \mu_B/\text{Mn}$ if only the magnetic moment of Mn ions is accounted for. In contrast, the Curie temperature (T_c), defined by the maximum of $|dM/dT|$, displays a significantly upward shift under magnetic fields. It is ~ 75 K for $H=0.8$ T and ~ 107 K for $H=5$ T (inset plot in the top panel of Fig. 1). The resistivity of ESMO is also presented in Fig. 1 as a function of temperature, and an excellent magnetic-resistive correspondence is observed as for the typical manganites. These results are similar to those observed by Sundaresan, Maignan, and Reveau in the compound of the same formula.¹⁰

Figure 2 presents the heat capacity (C_p) of ESMO measured under selected magnetic fields. The heat capacity exhibits a rapid increase with temperature. A visible step-like anomaly appears at ~ 95 K without magnetic field, which is a sign of AFM transition. It is surprising that there is no

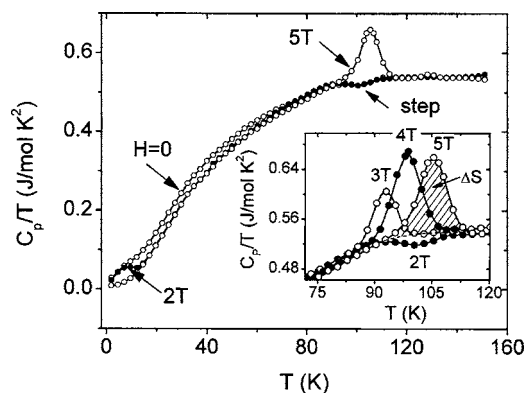


FIG. 2. Temperature-dependent heat capacity of $\text{Eu}_{0.58}\text{Sr}_{0.42}\text{MnO}_3$ measured under selected magnetic fields. Inset plot is a close view of the heat capacity around T_c . Hatched area marks the magnetic entropy change due to the FM transition. Solid lines are guides for the eye.

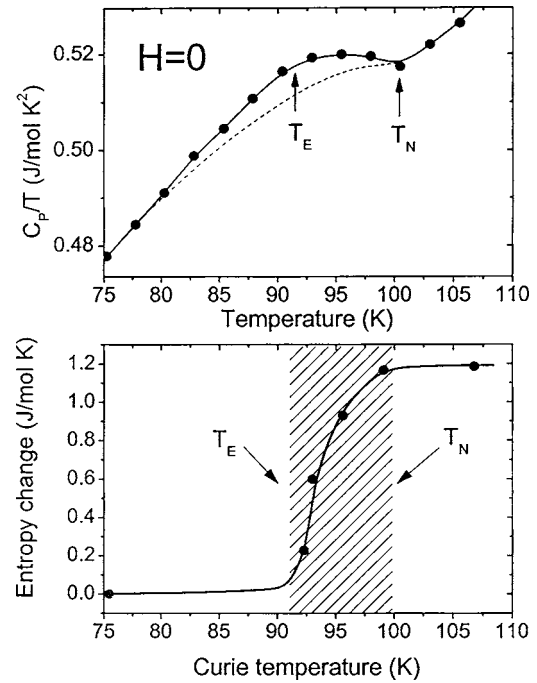


FIG. 3. Definition of the Néel temperature and the ending point for the AFM transition based on the data of heat capacity (top panel) and the magnetic entropy change as a function of Curie temperature (bottom panel). Dashed curve is the smooth background determined by a polynomial fitting. Solid lines are guides for the eye. Hatched area marks the temperature region for the AFM transition.

thermal response to the magnetic transition when the applied field is below 2.5 T, though both the magnetic and resistive measurements confirm the occurrence of FM transition. Thermal anomaly emerges when $H > 2.5$ T, increases rapidly with applied field, and reaches a saturation for $H > 4$ T (inset plot in Fig. 2).

A careful analysis shows that the heat capacity data recorded under $H=2$ T and 5 T, respectively, coincide with each other pretty well between 15 and 75 K, which confirms the FM structure of ESMO under the field of 2 T. The magnetic data in Fig. 1 indicate that the FM transition is rather sharp. This means that the absence of thermal response for $H < 2.5$ T cannot be due to a smooth entropy release for a broad FM transition. It may have the same origin as that observed in $\text{La}_{1-x-y}(\text{Pr}, \text{Nd})_x\text{Ca}_y\text{MnO}_3$ or $\text{Pr}_{1-x}\text{Ca}_x\text{MnO}_3$.

Based on the calorimetric data, the system experiences an AFM transition near ~ 95 K. As shown by the top panel of Fig. 3, this transition proceeds in a finite temperature range due to the presence of inhomogeneity probably associated with grain boundaries, and the step-like anomaly in the $C_p/T-T$ curve is actually an expansion of the λ -shaped transition. We define the concavity in the $C_p/T-T$ curve as the onset of the AFM transition (T_N) and the maximum, after subtracting the smooth background, as the ending of this transition (T_E). According to Fig. 1, the first identifiable Curie temperature is ~ 75 K. It is well below T_E . However, T_c sweeps through the AFM transition region with increasing field if T_N is independent of magnetic field, which is a reasonable assumption for the manganites. We noticed that the thermal anomaly appears only when $T_N > T_c > T_E$. A more quantitative description is given in the bottom panel of Fig. 3, in which the magnetic entropy change, calculated based on $\Delta S = \int_{\Delta T} \Delta C/T dT$, is illustrated as a function of the

Curie temperature, where ΔC is the magnetic contribution obtained by subtracting the lattice contribution (determined by fitting the background to a polynomial) from the total heat capacity, ΔT is the temperature span of the magnetic transition. It demonstrates that the thermal response emerges when T_c exceeds T_E , grows drastically as T_c sweeps from T_E to T_N , and saturates at ~ 1.2 J/mol K for $T_c > T_N$. The saturated ΔS value agrees with that observed in $\text{La}_{0.7}\text{Ca}_{0.3}\text{MnO}_3$ fairly well (~ 1.6 J/mol K), which indicates that ESMO behaves like an ordinary manganite above T_N .

In the case $T_c < T_E$ the system experiences a PM-AFM and an AFM-FM transition in sequence on cooling, whereas there is only one PM-FM transition for $T_c > T_N$. This suggests that the thermal response to magnetic ordering always occurs accompanying the PM-FM transition, and the magnetic contribution of the AFM-FM transition to heat capacity is ignorable. This analysis is consistent with the observation that the rapid increase of ΔS takes place only between T_E and T_N . It is possible that the AFM and PM phases coexist in this temperature range, and the volume fraction of the latter, thus the contribution of the PM-FM transition increases as T approaches T_N . There will be only the PM phase above T_N . As a result, the drastic increase of ΔS stops.

In fact, magnetic internal energy exists no matter whether the system is at the AFM or the FM state. It has been well established that the exchange energy has the form $\varepsilon \propto \lambda M^2$, where M is the magnetization of the system and λ the magnetic coupling between magnetic ions. A direct calculation shows that the contribution of the AFM-FM transition to heat capacity will be $\Delta C = (\lambda_{\text{AF}} M_{\text{AF}}^2 - \lambda_{\text{FM}} M_{\text{FM}}^2) df/dT$, where f is the volume fraction of the FM phase. $(\lambda_{\text{AF}} M_{\text{AF}}^2 - \lambda_{\text{FM}} M_{\text{FM}}^2)$ is the difference of the exchange energy in the AFM and the FM states. It must be smaller than $2M_{\text{FM}}$ noting the fact that a field of 2 T can stabilize the FM state effectively. This actually implies that $\Delta C/C < 2M_{\text{FM}}/\lambda_{\text{FM}} M_{\text{FM}}^2 < 1/40$, where the inequality $\lambda_{\text{FM}} M_{\text{FM}} > 80$ T has been used considering the fact that the Curie temperature of ESMO is ~ 80 K under a field of 2 T. That is, the change in heat capacity due to an AFM-FM transition will only be one fortieth of that of a PM-FM tran-

sition. This may be the reason for the absence of thermal response to an AFM-FM transition.

In a similar picture we can understand the experiment results obtained for $\text{Pr}_{1-x}\text{Ca}_x\text{MnO}_3$ and $\text{La}_{1-x-y}(\text{Pr}, \text{Nd})_x\text{Ca}_y\text{MnO}_3$. For $\text{Pr}_{0.63}\text{Ca}_{0.37}\text{MnO}_3$ the PM-AFM and AFM-FM transitions take place, respectively, at ~ 170 and 100 K.⁸ Similarly, the FM transition is ~ 80 K below the AFM-PM transition for $\text{La}_{1-x-y}(\text{Pr}, \text{Nd})_x\text{Ca}_y\text{MnO}_3$. These mean that the FM transition in these compounds is actually an AFM-FM transition, which explains the absence of thermal anomaly in heat capacity. However, if the long range AFM order is partially destroyed by, for example, element doping, the field-induced phase transition will be an incomplete AFM-FM transition, and entropy changes could occur. This was demonstrated by the work of Hardy *et al.* for $\text{Pr}_{0.5}\text{Ca}_{0.5}\text{Mn}_{0.95}\text{Ga}_{0.05}\text{O}_3$.⁹

This work has been supported by the National Natural Science Foundation of China and the State Key Project for the Fundamental Research of China.

¹For a review, see *Colossal Magnetoresistance, Charge Ordering, and Related Properties of Manganese Oxides*, edited by C. N. R. Rao and B. Raveau (World Scientific, Singapore, 1998); *Physics of Manganites*, edited by T. A. Kaplan and S. D. Mahanti (Kluwer Academic/Plenum, New York, 1999); *Colossal Magnetoresistance Oxides*, edited by Y. Tokura (Gordon and Breach, London, 1999).

²C. Zener, Phys. Rev. **81**, 440 (1951).

³P. W. Anderson and H. Hasegawa, Phys. Rev. **100**, 675 (1955).

⁴K. Kubo and N. Ohata, J. Phys. Soc. Jpn. **33**, 21 (1970); J. Tanaka and T. Mitsuhashi, *ibid.* **53**, 24 (1980).

⁵G.-L. Liu, J.-S. Zhou, and J. B. Goodenough, Phys. Rev. B **64**, 144414 (2001); Phys. Rev. B **70**, 224421 (2004).

⁶G. H. Rao, J. R. Sun, J. K. Liang, and W. Y. Zhou, Phys. Rev. B **55**, 3742 (1997); K. H. Kim, M. Uehara, C. Hess, P. A. Sharma, and S.-W. Cheong, Phys. Rev. Lett. **84**, 2961 (2000).

⁷V. Kiryukhin, B. G. Kim, V. Podzorov, and S.-W. Cheong, Phys. Rev. B **63**, 024420 (2000).

⁸A. K. Raychaudhuri, A. Guha, I. Das, R. Rawat, and C. N. R. Rao, Phys. Rev. B **64**, 165111 (2001).

⁹V. Hardy, A. Maignan, S. Hebert, and C. Martin, Phys. Rev. B **67**, 024401 (2003).

¹⁰A. Sundaresan, A. Maignan, and B. Reveau, Phys. Rev. B **55**, 5596 (1997).